Highly efficient submonolayer Pt-decorated Au nano-catalysts for formic acid oxidation†

Noel Kristian,[a] Yushan Yan[b] and Xin Wang*[a]

Received (in Cambridge, UK) 14th September 2007, Accepted 23rd October 2007
First published as an Advance Article on the web 31st October 2007
DOI: 10.1039/b714230g

A novel structure of catalyst, submonolayer Pt-decorated Au, has been synthesized with minimal use of Pt and shows markedly improved activity toward formic acid oxidation where it facilitates the direct oxidation of formic acid by suppressing the formation of poisonous species CO_{ads} *via* the "ensemble" effect.

Lately formic acid has received a growing attention because the direct formic acid fuel cell (DFAFC) has several advantages over the direct methanol fuel cell including higher theoretical open circuit potential and lower fuel crossover.[1] With Pt as the most commonly used electrocatalyst, previous publications have shown that formic acid oxidation on Pt follows a dual path mechanism, *i.e.* a dehydrogenation path and a dehydration path, and adsorption of intermediate CO from the dehydration path greatly hinders its activity.[2] The mitigation of the CO poisoning phenomenon has been attempted by alloying Pt with other metals[3] or using a Pd based catalyst.[4] However, the effect of such alloying is limited and some are investigated in the bulk alloy phase which does not represent the real behaviour of the nano-catalyst. More importantly, the amount of Pt or Pd used in a DFAFC is still considered too much for commercial applications. More efforts are needed for the development of a new electrocatalyst with lower cost and higher activity. So far little attention has been paid to the deposition of a submonolayer amount of Pt on the surface of another metal. In this communication, we have successfully prepared Pt-decorated Au on carbon black support as a novel electrocatalyst for formic acid oxidation. This catalyst not only significantly reduces the use of Pt *via* improved Pt dispersion, but also shows a markedly high activity toward formic acid oxidation. Compared to Pt/C, it undergoes a different reaction pathway by suppressing the formation of the CO poisoning intermediate where the Pt coverage on Au nanoparticles plays an important role. To the best knowledge of the authors, it is the first time that a Pt based nano-electrocatalyst is reported to effectively block the CO formation branch while the amount of Pt needed is markedly reduced.

The Au hydrosol was prepared based on the previous reported protocol by Grabar *et al.*[5a] The successful reduction of the $AuCl_4^-$ to Au hydrosol was verified by UV-Vis spectroscopy. As shown in Fig. 1A, the strong absorption peak at 294 nm is attributed to the absorption of $AuCl_4^-$ near the red region wavelength.[6a] Before the reaction this peak could be observed but after only 7 min of reaction (dashed line), this absorption peak vanished. Instead, a weak absorption peak at 511 nm that belongs to Au hydrosol was observed.[6a,6b] The TEM observation reveals that the final size of the Au hydrosol was 4.8 nm with a spherical shape (see Fig. S1 in the ESI†).

The decoration of Pt onto Au seeds was realized by $NH_2OH{\cdot}HCl$ reduction of H_2PtCl_6 to Pt in the presence of Au seed (see ESI†). This reducing agent was carefully chosen as it is known that $NH_2OH{\cdot}HCl$ acts only as a growth agent in slightly acid environments without forming new nuclei.[7] By changing the Pt : Au mole ratio which is less than the ratio needed to make one complete monolayer shell, a controllable Au surface coverage can be achieved. Here we have successfully prepared a Pt-decorated Au electrocatalyst, with a Pt : Au mole ratio ranging from 1 : 6 to 1 : 2. The UV-Vis results in Fig. 1B show that there's a continuous blue shift and suppression of the Au plasmon peak with an increase in the Pt : Au mole ratio. This can be explained by the decreasing exposed Au surface area which leads to a broader and lower Au plasmon peak.[6] Liz-Marzan and Philipse have reported that, based on the modified Mie theory for the Au_{core}–Pt_{shell} case, the Au plasmon absorption peak became suppressed with the increase of surface coverage and finally vanished when a complete Pt monolayer was formed.[6c] This is in good agreement with our experimental result. Because the Au plasmon absorption is related directly to the exposed Au surface area, we suggest that by

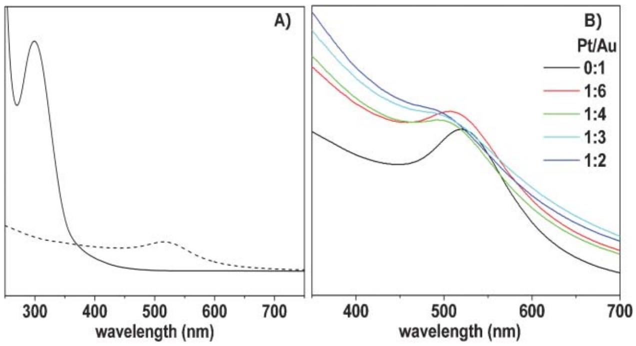

Fig. 1 (A) UV-Vis spectra of precursor solution (——) and Au hydrosol after 7 min of reaction (---). (B) UV-Vis spectra of PtAu hydrosols with different Pt : Au mole ratios.

---

[a] *School of Chemical and Biomedical Engineering, Nanyang Technological University, Singapore, 637459. E-mail: WangXin@ntu.edu.sg; Fax: +65 6794 7553; Tel: +65 6316 8866*
[b] *College of Engineering – Center for Environmental Research and Technology (CE-CERT) and Department of Chemical and Environmental Engineering, University of California, Riverside, CA 92521, USA*

† Electronic supplementary information (ESI) available: Preparation procedures, characterization techniques and results. See DOI: 10.1039/b714230g

comparing the Au plasmon peak area from the UV-Vis spectrum, the surface coverage of Au by Pt can be semi quantitatively predicted. The estimated surface coverage changes from 20% to 87% when the Pt : Au ratio changes from 1 : 6 to 1 : 2 (see Table S1 in the ESI†). It is interesting to note that the estimated surface coverage of 87% for the ratio of 1 : 2 agrees well with the surface coverage (86%) calculated by assuming epitaxial growth of Pt on the 4.8 nm Au.

The average size of the final products is around 5 nm based on the TEM observations (Fig. 2 and Fig. S1†). This number is slightly greater than the size of the Au core which is 4.8 nm. This suggests that all Pt is deposited on the Au surface, not forming individual particles. Since less than one monolayer of Pt is formed, the size difference between different Pt : Au ratios is negligible. We tried to do HRTEM for the PtAu mole ratio 1 : 3 in order to obtain a clear difference between the Au and Pt fringe on the edge of the particle (Fig. 2B), but due to the small difference in lattice constant and imaging contrast, this feature cannot be observed even at high magnification.

All the XRD spectra for the Pt-decorated Au resemble the Au spectra where all the (111), (200), (220) and (311) peaks can be observed (see Fig. S2 in the ESI†). This indicates that only a monolayer or sub-monolayer of Pt was deposited on Au without forming individual Pt particles, otherwise the XRD spectrum would have replicated the Au and Pt peaks as of a physical mixture.[6b,6e] The absence of Pt peaks implies that the size of the Pt clusters on the surface of Au are smaller than the detecting capability of XRD (~1 nm). This XRD analysis agrees well with the TEM observation.

The formation of this decorated structure is further supported by electrochemical measurements. Cyclic voltammograms of the Pt-decorated Au on a Vulcan XC-72 in deaerated 0.5 M H_2SO_4 exhibit the same characteristic as Pt/C where the H adsorption–desorption and the Pt oxide reduction peak are well observed (see Fig. S3 in the ESI†).[8] From the zoom-in of the cathodic scan (see Fig. S4 in the ESI†), for the PtAu/C with a Pt : Au ratio from 1 : 6 to 1 : 2, the Au oxide reduction peak at ~0.9 V still can be observed but it becomes increasingly suppressed with an increasing amount of Pt. When the Pt : Au ratio is raised to 1 : 1 and above, the Au oxide reduction peak completely disappeared. This reveals that Pt is deposited onto the Au surface instead of forming its own nucleus. When the Pt : Au ratio is not high enough to form complete coverage, some of the Au surface is still not covered with Pt, giving a decorated structure.

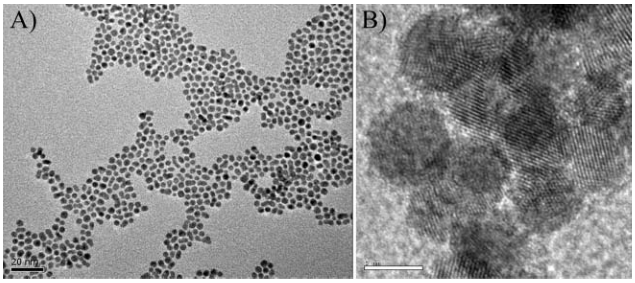

Fig. 2 (A) TEM image of PtAu (Pt : Au = 1 : 4). (B) HRTEM image of PtAu (Pt : Au = 1 : 3); scale bar is equal to 20 and 5 nm for (A) and (B) respectively.

What is of interest is the unprecedented high activity this decorated structure exhibited for formic acid oxidation. Fig. 3 shows the voltammograms of Au/C, Pt/C, PtAu/C (Pt : Au = 1 : 2) which has a decorated structure, and PtAu/C (Pt : Au = 1 : 1) which is of a core–shell structure in 0.5 M formic acid. It is clear that Au/C itself has negligible activity towards formic acid oxidation. For Pt/C, two peaks were observed in the forward scan. Instead of the backward scan, we focus our observation on the evolution of anodic current during the forward scan, as the latter allows the poisoning species to accumulate on the Pt surface, which is closer to the real situation. It is well known that dual parallel reaction paths exist for formic acid oxidation, *i.e.*, a dehydrogenation step to form CO_2 and a dissociative adsorption to form poisoning CO species. The first peak at ~0.34 V on the Pt/C voltammogram is related to the direct oxidation of HCOOH to form CO_2 while the second peak at ~0.63 V is related to the oxidation of the CO_{ads} generated from the dissociative adsorption step.[1,2a,9] The intensity of these two peaks gives an indication of along which path the reaction is proceeding. It can be seen that the core–shell structure showed slightly higher activity than Pt/C with a similar peak shape and intensity, indicating a similar reaction mechanism. Interestingly the decorated structure (Pt : Au = 1 : 2) showed a remarkable increase in the activity where the first peak at 0.3 V became higher compared to the Pt/C and the core–shell catalyst. This indicates that the formic acid oxidation on the decorated catalyst shifts towards the dehydrogenation branch. During the backward scan, all the poisoning species have been oxidized at high potential and formic acid oxidation then can occur on the clean Pt surface. This is why the backward peak current is always higher than the forward peak current for the catalysts which form a significant amount of poisoning species, like Pt/C, PtAu core–shell, or PtAu with a high ratio (1 : 2), as more Pt sites are released by the oxidation of CO_{ads} during the high potential of backward scan.

Even more interesting is the result of the Pt-decorated Au with a lower Pt : Au ratio, where the second peak completely vanished as shown in Fig. 4. The measured currents of the decorated structure do not appreciably differ for the anodic and cathodic scan, indicating a low inhibition rate, *i.e.*, a low tendency toward CO formation.[9c] Instead, Pt/C and the Pt–Au core–shell catalyst show

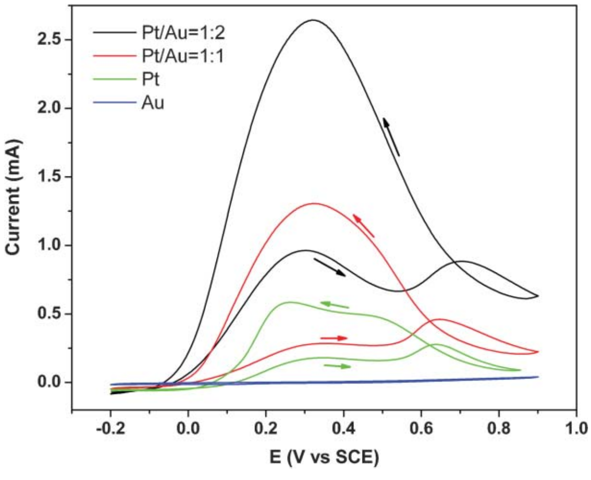

Fig. 3 Cyclic voltammograms (CV) of Au/C, Pt/C and PtAu/C (core–shell and decorated) at 10 mV s^{-1} in 0.5 M HCOOH + 0.5 M H_2SO_4.

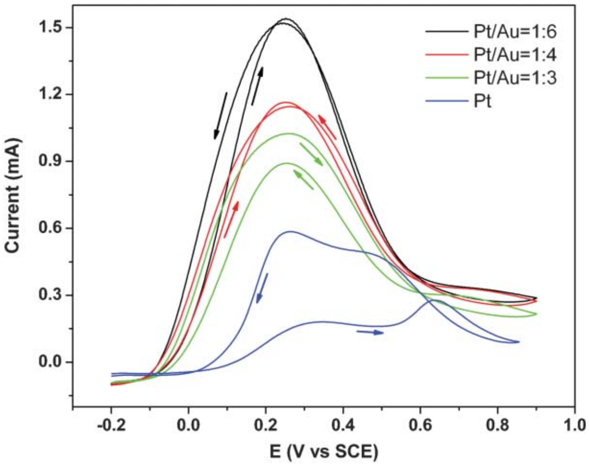

Fig. 4 CV of Pt/C and PtAu/C at 10 mV s^{-1} in 0.5 M HCOOH + 0.5 M H_2SO_4.

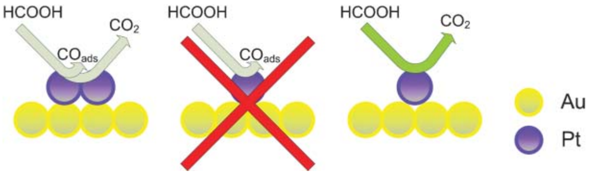

Scheme 1 Illustration of the catalytic reactions of formic acid oxidation (dissociative adsorption and dehydrogenation) on the Pt-decorated Au surface.

a large difference between forward and backward scan, suggesting the severe poisoning of catalytic sites by CO. These observations suggest that the dehydration branch to form CO_{ads} is mostly suppressed on the Pt-decorated Au with a Pt : Au ratio below 1 : 3 and the majority of the formic acid is oxidized *via* a dehydrogenation step. This catalytic behaviour is very similar to the catalytic behaviour of Pd/C toward formic acid oxidation where Pd facilitates the formic acid oxidation *via* the dehydrogenation step without forming the strongly adsorbed intermediates (CO_{ads}).[4,9d,9e]

A clear view on the enhancement originating from the decorated structure can also be obtained from the lower onset potential (−0.1 V *vs.* 0 V for Pt/C). A lower onset potential for the decorated structure means that the formic acid is easier to oxidize. Moreover, the anodic peak current increases surprisingly with the decrease in the Au surface coverage by Pt, suggesting that the catalytic capabilities of the Pt atoms actually improved with the decrease in the coverage within the range studied. This enhancement can be due to either the fast and facile removal of CO adsorbed on Pt surfaces through the ligand effect or by the suppression of CO formation on Pt surfaces. The former does not agree with the theoretical calculation and experimental results where a stronger Pt–CO_{ads} bond was confirmed by DFT calculations,[10] CO electrooxidation[11] and temperature programmed desorption (TPD) on chemisorbed CO[12] on submonolayer Pt deposited on the Au surface. The latter seems the only possible reason, which can be explained by the "ensemble" effect as illustrated in Scheme 1. It is believed that the direct oxidation of formic acid on Pt surface (dehydrogenation) does not require the presence of continuous neighbouring Pt sites, while the dissociative adsorption of formic acid to form CO requires at least two ensemble binding sites.[2b] A continuous decrease in Pt coverage on the Au surface, *i.e.*, decreasing the availability of adjacent Pt atoms, leads to a decrease in the dehydration rate and an eventual blocking of CO formation (the disappearance of the second oxidation peak at ~0.63 V), while the dehydrogenation reaction can still occur without being affected.

Finally, it is worthwhile to mention that these measured oxidation currents are reported based on the same total metal loading. Considering that the amount of Pt used in the decorated catalyst is much less than in conventional Pt/C, the improved Pt utilization is clearly exemplified with the decorated structure, *e.g.*, at a potential of 0.3 V, PtAu/C (Pt : Au = 1 : 6) exhibits a current 5 times higher than Pt/C while the amount of Pt used is only 14.3% of Pt/C.

This work is supported by the Startup-grant of Nanyang Technological University, Academic research fund AcRF tier 1(RG40/05) and AcRF tier 2 (ARC11/06), Ministry of Education, Singapore. The authors wish to thank Mr P. Gunawan and S. Y. Wang for helping with the TEM analysis.

Notes and references

1 X. Wang, J. M. Hu and I. M. Hsing, *J. Electroanal. Chem.*, 2004, **562**, 73.
2 (*a*) J. D. Lovic, A. V. Tripkovic, S. Lj. Gojkovic, K. Dj. Popovic, D. V. Tripkovic, P. Olszewski and A. Kowal, *J. Electroanal. Chem.*, 2005, **581**, 294; (*b*) S. Park, Y. Xie and M. J. Weaver, *Langmuir*, 2002, **18**, 5792; (*c*) S. C. Chang, L. W. H. Leung and M. J. Weaver, *J. Phys. Chem.*, 1990, **94**, 6013.
3 (*a*) L. J. Zhang, Z. Y. Wang and D. G. Xia, *J. Alloys Compd.*, 2006, **426**, 268; (*b*) W. Chen, J. Kim, S. Sun and S. Chen, *Phys. Chem. Chem. Phys.*, 2006, **8**, 2779; (*c*) Y. J. Leng, X. Wang and I. M. Hsing, *J. Electroanal. Chem.*, 2002, **528**, 145.
4 (*a*) W. P. Zhou, A. Lewera, R. Larsen, R. I. Masel, P. S. Bagus and A. Wieckowski, *J. Phys. Chem. B*, 2006, **110**, 13393; (*b*) H. Li, G. Sun, Q. Jiang, M. Zhu, S. Sun and Q. Xin, *Electrochem. Commun.*, 2007, **9**, 1410.
5 (*a*) K. C. Grabar, K. J. Allison, B. E. Baker, R. M. Bright, K. R. Brown, R. G. Freeman, A. P. Fox, C. D. Keating, M. D. Musick and M. J. Natan, *Langmuir*, 1996, **12**, 2353; (*b*) W. Li, C. Liang, W. Zhou, J. Qiu, Z. Zhou, G. Sun and Q. Xin, *J. Phys. Chem. B*, 2003, **107**, 6292; (*c*) T. J. Schmidt, H. A. Gasteiger, G. D. Stab, P. M. Urban, D. M. Kolb and R. J. Behm, *J. Electrochem. Soc.*, 1998, **145**, 2354.
6 (*a*) S. Nath, S. Praharaj, S. Panigrahi, S. K. Ghosh, S. Kundu, S. Basu and T. Pal, *Langmuir*, 2005, **21**, 10405; (*b*) T. Yonezawa and N. Toshima, *J. Chem. Soc., Faraday Trans.*, 1995, **91**, 4111; (*c*) L. M. Liz-Marzan and A. P. Philipse, *J. Phys. Chem.*, 1995, **99**, 15120; (*d*) C. Kan, W. Cai, C. Li, L. Zhang and H. Hofmeister, *J. Phys. D: Appl. Phys.*, 2003, **36**, 1609; (*e*) M.-L. Wu, D.-H. Chen and T.-C. Huang, *Chem. Mater.*, 2001, **13**, 599.
7 (*a*) S. Schmid, A. Lehnert, J.-O. Malm and J.-O. Bovin, *Angew. Chem., Int. Ed. Engl.*, 1991, **30**, 874.
8 S. H. Yoo and S. Park, *Adv. Mater.*, 2007, **19**, 848.
9 (*a*) A. Capon and R. Parsons, *J. Electroanal. Chem.*, 1973, **44**, 1; (*b*) A. Capon and R. Parsons, *J. Electroanal. Chem.*, 1973, **45**, 205; (*c*) M. Baldauf and D. M. Kolb, *J. Phys. Chem.*, 1996, **100**, 11375; (*d*) A. Capon and R. Parsons, *J. Electroanal. Chem.*, 1973, **44**, 239; (*e*) X. Li and I.-M. Hsing, *Electrochim. Acta*, 2006, **51**, 3477; (*f*) G.-Q. Lu, A. Crown and A. Wieckowski, *J. Phys. Chem. B*, 1999, **103**, 9700.
10 C. Song, Q. Ge and L. Wang, *J. Phys. Chem. B*, 2005, **109**, 22341.
11 K. A. Friedrich, F. Henglein, U. Stimming and W. Unkauf, *Electrochim. Acta*, 2000, **45**, 3283.
12 M. Ø. Pedersen, S. Helveg, A. Ruban, I. Stensgaard, E. Lægsgaard, J. K. Nørskov and F. Besenbacher, *Surf. Sci.*, 1999, **426**, 395.